Commun. Comput. Phys.
doi: 10.4208/cicp.2009.09.044

Vol. 7, No. 4, pp. 718-737
April 2010

Simulation of Decoherence by Averaged Semiquantum Method

Zhuo Wang*, Quanlin Jie and Shi-Hui Zhang

Department of Physics, Wuhan University, Wuhan 430072, China.

Received 2 March 2009; Accepted (in revised version) 12 August 2009

Communicated by Michel A. Van Hove

Available online 12 October 2009

Abstract. We investigate the dynamics of a system coupled to an environment by averaged semiquantum method. The theory origins from the time-dependent variational principle (TDVP) formulation and contains nondiagonal matrix elements, thus it can be applied to study dissipation, measurement and decoherence problems in the model. In the calculation, the influence of the environment governed by differential dynamical equation is incorporated using a mean field. We have performed averaged semiquantum method for a spin-boson model, which reproduces the results from stochastic Schrodinger equation method and Hierarchical approach quite accurately. Moreover, we validate our results with noninteracting-blip approximation (NIBA) and generalized Smoluchowski equation (GSE). The problem dynamics in nonequilibrium environments has also been studied by our method. When applied to the harmonic oscillator model coupled to a heat bath with different coupling strengths and dimensionalities of the bath, we find that the loss of coherence predicted by semiquantum method is identical to the result of master equation with different initial state (Gaussian wave packet and superposed wave packets).

PACS: 05.45.Mt, 03.65.Yz, 03.65.Ud

Key words: Quantum chaos, spin-boson model, decoherence, harmonic oscillator system, environment, averaged semiquantum method.

1 Introduction

The system-bath dynamics of open quantum systems at finite temperatures has long been a central problem in chemistry and physics [1, 2], which is usually associated with reduced density matrix evolving in time according to the Liouville von-Neumann equation. The understanding of the nonequilibrium dynamics of open quantum systems has also

*Corresponding author. *Email addresses:* wangzhuoxxh@yahoo.com.cn (Z. Wang), qljie@whu.edu.cn (Q. Jie), shihuizhang@yahoo.cn (S.-H. Zhang)

been a main challenge in the last decades [3]. In recent years the subject has particularly gained considerable interest due to experimental progress which allows for the tailoring and manipulation of quantum matter on ever larger scales. In mesoscopic physics, for instance, superconducting circuits have been realized to observe coherent dynamics and entanglement [4]. Similar advance has been achieved on molecular scales with the detection of interferences in wave packet dynamics and the control of the population of specific molecular states [5]. These systems are in contact with a large number of environmental degrees of freedom, giving rise to decoherence and relaxation [6].

Traditional approaches treating the dynamics typically yield approximate equations of motion such as master equations. For large coupling constants and long time scales, it can be accomplished in a formally exact manner by path integrals for open quantum systems [7]. Noninteracting-blip approximation (NIBA) was originally derived by Leggett using the path-integral influence-functional method [35], and can be obtained using standard reduced density matrix perturbation theory by Aslagul *et al.* [36]. Generalized Smoluchowski equation (GSE) was introduced by Zusman [37] and later derived by Garg *et al.* [38].Very recently, it was generalized to study electron-transfer problem [39]. Furthermore, Monte Carlo wave-function techniques [8–14] are extensively used to treat master equations in the weak coupling or Markovian limit. In recent years, the quantum dynamics in nonequilibrium environments has attracted our attention. Also, stochastic equation [15–18] is used to treat the system-environment problem, which can describe the long-time evolution exactly.

In this work, we propose averaged semiquantum method to study the system environment problem. Conventional semiquantum method has a wide application in many branches of physics. Recently, this method has been used to study the nonlinear dynamics and chaos [19]. It is also named as Gaussian wave-packet dynamics [20, 21] and origins from TDVP formulation, $\Gamma=\int dt\langle\Psi(t)|i\hbar\frac{\partial}{\partial t}-\hat{H}|\Psi(t)\rangle$ with $\delta\Gamma=0$. This approach enables us to study the effects of the quantum fluctuations dynamically [22–23]. Moreover it has been proven to be very successful in the investigation of dynamical systems ranging from integrable to many-body nonintegrable systems [24], which simplifies the quantum version and gives better results than the semiclassical approach. The averaged semiquantum method may provide a significant numerical advantage over the trajectories, in particular in the case that the Hilbert space dimension$N$ of the open system is large. Moreover, to be numerically efficient (the best possible sampling), it gives good solutions with a significant weight in average.

The spin-boson model [40] and the harmonic oscillators system [41] have been the subject of considerable attention with a major review available. In this paper, at first, we focus on the spin-boson system and compare the results with that obtained by the stochastic Schrodinger equation method. Then we study the harmonic oscillator model coupled to a heat bath with different dimensionalities to find whether the loss of coherence can be predicted by the semiquantum method.

The paper is organized as follows: In Section 2 we introduce the averaged semiquantum method. In Section 3 we will use this method to study the spin-boson model and

compare with other methods. In Section 4 we will further use this method to study the harmonic oscillators system and compare the results with those from other methods. Finally, we draw conclusions.

2 Averaged semiquantum method

In this part, we obtain an equation of motion for the reduced system dynamics, and the environment effect is incorporated through a mean field. We consider here a system (S)-environment (E) described by a Hamiltonian

$$H = h_S + h_E + h_I, \tag{2.1}$$

where h_S is the Hamiltonian for the system which consists of a few degree of freedom, h_E the Hamiltonian for the bath which consists of large number of degrees of freedom, and h_I is the coupling. Here we assume that the interaction is written as

$$h_I = Q \otimes B, \tag{2.2}$$

where $Q \equiv \{q_i^s\}_{i=1,\cdots,n_s} B \equiv \{q_i\}_{i=1,\cdots,n_B}$, corresponding to functions of two sets of operators of the system and environment, respectively. Averaged semiquantum method to the study of time-dependent quantum dynamics origins from the result of the variational principle

$$\langle \delta\psi | i\hbar\partial_t - H_I | \psi \rangle = 0. \tag{2.3}$$

The wave function is represented as

$$|\psi\rangle = |\psi_0\rangle \prod_{k=1}^{N} |\psi_k\rangle, \tag{2.4}$$

where $|\psi_k\rangle$ is the single-particle wave function for kth degree of freedom of the bath and $N$is the total number of degrees of freedom. $|\psi_0\rangle$ is the wave function for the system. Furthermore,we choose the Gaussian wave packet, which is widely used in the semiquantum method, to describe.

$$|\psi_k\rangle = (2\pi\hbar\bar{G}_k)^{-1/4} \exp\left[-\frac{1}{2\hbar}(q-\bar{q}_k)^2 \left(\frac{1}{2}\bar{G}_k^{-1} - 2i\bar{\prod}_k\right) + i\bar{p}_k(q-\bar{q}_k)/\hbar \right], \tag{2.5}$$

where $\bar{G}_k$, $\bar{\prod}_k$, $\bar{q}_k$ and $\bar{p}_k$ are all time-dependent.

The initial conditions of the bath can be sampled from the Wigner distribution at the saddle points, or from the classical action-angle variables

$$\begin{aligned} &G_k(0) = 1/2a_k\hbar, \\ &\Pi_k(0) = 0, \\ &q_k^{inital}(0) = \sqrt{2n_k+1}\sin b_k + \delta_k, \\ &p_k^{inital}(0) = \sqrt{2n_k+1}\cos b_k, \end{aligned} \tag{2.6}$$

where the phases b_k are picked randomly from the interval $[0,2\pi]$, the quantum numbers n_k are sampled according to the Boltzmann distribution

$$P(n_k)=\exp(-\beta n_k\omega_k).$$

The coordinate shift δ_k (nonequilibrium parameters) reflects the initial mean position of the bath modes. $a_k^{-1/2}$equals the width of the coherent state of a corresponding harmonic oscillator. In [42], Section 1 derive an arbitrary expression for the thermal width

$$a_k=\frac{m_k\omega_k}{\hbar}\Big[\coth(\frac{\hbar\omega_k}{2k_BT})-\frac{2k_BT}{\hbar\omega_k}\Big]^{-1}.$$

We use

$$\begin{aligned}
&q_k^j=q_k^{inital}-a_k^{-1/2}+j*\Delta q, \quad \Delta q=\frac{2*a_k^{-1/2}}{N_k},\\
&p_k^j=p_k^{inital}-\frac{\pi\hbar}{\Delta q}+j*\Delta p, \quad \Delta p=\frac{2\pi\hbar}{\Delta q*N_k}=\pi\hbar a_k^{1/2},\\
&\qquad j=0,\cdots,N_k,
\end{aligned} \tag{2.7}$$

to sample the initial conditions of the trajectories around the central point q_k^{inital} and p_k^{inital}. N_k is the sampling number.

C_j^m, the distribution of initial conditions for the trajectory, is given by

$$\begin{aligned}
&C_j^m=\prod_{m=1}^{N}w_m(p_m,q_m),\\
&\quad w_m(p_m,q_m)=w_m(p_m)*w_m(q_m),\\
&\quad w_m(q_m)=(2\pi\hbar G_m)^{-1/2}\exp\Big[-\frac{1}{2\hbar G_m}(q_m-q_m(0))^2\Big]*\Delta q,\\
&\quad w_m(p_m)=(2\hbar G_m/\pi)^{-1/2}\exp[-2\hbar G_m(p_m-p_m(0))^2]*\Delta p,
\end{aligned} \tag{2.8}$$

where N is the degree of dimensionality.

From (2.5) to (2.8), we can find that our method is quite different from the conventional semiquantum method. The semiquantum method only takes into account the central point $(q_k^{inital},p_k^{inital})$, and does not consider other points (q_m,p_m). The effect from the points around the central point is ignored. In our method, we not only consider the point (q_k^j,p_k^j), but also consider its own weights. In (2.5), we introduce the average Gaussian wave packet to represent the wave function. This is the reason why we call our method as the averaged semiquantum method. All semiquantal quantities are obtained by evaluating each individual trajectory and averaging them, taking into account their respective probabilities.

Substituting (2.4) into (2.3), we can obtain the averaged semiquantum method working equations, using Gaussian integration. From the interaction Hamiltonian, the associated mean-field dynamics can be obtained according to the variational principle. The influence of the environment on the system only enters through

$$\langle B(t)\rangle_E = -\sum k_n \langle q(t)\rangle. \tag{2.9}$$

Thus the introduction of the mean field to the interaction simplifies the version of the coupled model. For the spin-boson model, we use the form

$$|\psi_0\rangle = a(t)|0\rangle + b(t)|1\rangle \tag{2.10}$$

to perform calculation. In harmonic oscillators mode, we represent $|\psi_0\rangle$ as the Gaussian wave packet.

The averaged Semiquantum method is obtained by propagating each Gaussian wave packets, using the TDVP for each individual packet. This method can track the classical distribution even when the distribution is highly non-Gaussian and involves quantum coherence in phase space. Furthermore, it contains nontrivial quantum information. In this sense, it is not a semiclassical approximation. Using these, we can calculate our interested quantities to measure decoherence. All semiquantal quantities are obtained by evaluating each individual trajectory and averaging them, taking into account their respective probabilities. This averaged method is intuitionistic to describe the bath. In our method, we can use the parameter δ to describe the initial conditions of the non-equilibrium environment. This suggests that the averaged semiquantum can be used to simulate the bath with non-equilibrium initial conditions.

Except for the variational principle, no approximations are made to obtain equations. Therefore we can study the reduced density matrix by averaging over different paths. We use the decoherence function to measure decoherence of the averaged semiquantum version. Following [25–26], we consider the direct product of the system S and bath B Hilbert spaces. The system space is assumed to be N dimensional. We consider N orthogonal states ϕ_i^S of the system and a system-bath interaction that induces quantum transitions in the combined system, with the bath state responding to that of the system:

$$|\psi\rangle = |\psi_0\rangle \prod_{k=1}^{N} |\psi_k\rangle = \left(\sum_i c_i \left|\phi_i^S\right\rangle\right) \left|\phi_0^B\right\rangle \to \sum_i c_i \left|\phi_i^S\right\rangle \left|\phi_i^B\right\rangle = |\Psi_t\rangle, \tag{2.11a}$$

$$\left|\phi^B\right\rangle = \sum_{j=1}^{M} C_j \left|\psi_k^j\right\rangle, \tag{2.11b}$$

where ϕ_0^B is the initial state of the bath. Transitions from an arbitrary initial system $\sum_i c_i \phi_i^S$

are then described in terms of the reduced density matrix:

$$\begin{pmatrix} |c_1|^2 & \cdots & c_1c_i^* & \cdots & c_1c_N^* \\ \vdots & \ddots & \vdots & \iddots & \vdots \\ c_ic_1^* & \cdots & |c_i|^2 & \cdots & c_ic_N^* \\ \vdots & \iddots & \vdots & \ddots & \vdots \\ c_Nc_1^* & \cdots & c_Nc_i^* & \cdots & |c_N|^2 \end{pmatrix}$$

$$\rightarrow \begin{pmatrix} |c_1|^2 & \cdots & c_1c_i^*(\phi_i^B|\phi_1^B) & \cdots & c_1c_N^*(\phi_N^B|\phi_1^B) \\ \vdots & \ddots & \vdots & \iddots & \vdots \\ c_ic_1^*(\phi_1^B|\phi_i^B) & \cdots & |c_i|^2 & \cdots & c_ic_N^*(\phi_N^B|\phi_i^B) \\ \vdots & \iddots & \vdots & \ddots & \vdots \\ c_Nc_1^*(\phi_1^B|\phi_N^B) & \cdots & c_Nc_i^*(\phi_i^B|\phi_N^B) & \cdots & |c_N|^2 \end{pmatrix}. \tag{2.12}$$

Decoherence is defined as decay of the nondiagonal matrix elements, which is clearly determined by the decay of the sum of the inner product of the bath states $\sum_{i\neq j}(\phi_i^B\left|\phi_j^B\right.)$. Within the frozen Gaussian formulation [27], the decay of the integral and corresponding nondiagonal matrix elements is described by the decoherence function given by Eq. (39) of [28]. The decoherence function in the frozen Gaussian approximation is completely determined by the real valued nuclear overlap integral.

$$\begin{aligned} D(t) &= 1-\sum_{i\neq j}\left| c_jc_i^*(\phi_i^B\left|\phi_j^B\right.)\right| \approx 1-\sum_{i\neq j}\left| c_jc_i^*J_{overlap}(t)\right| \\ &= 1-\sum_{i\neq j}c_jc_i^*\prod_n \exp\Big(-0.25(\bar{q}_{jn}(t)-\bar{q}_{in}(t))^2/\bar{G}_n\Big)\times\exp\Big(-0.25*\bar{G}_n(\bar{p}_{jn}(t)-\bar{p}_{in}(t))^2/\hbar^2\Big) \\ &\quad\times\cos\Big(-0.5(\bar{q}_{jn}(t)-\bar{q}_{in}(t))(\bar{p}_{jn}(t)+\bar{p}_{in}(t))/\hbar\Big), \end{aligned} \tag{2.13}$$

where $\bar{h}$ means the statistic average time-dependent physical quantity h along its trajectory in phase space.

To treat the continuum spectrum of the harmonic oscillators bath modes, we use frequencies density $\rho(\omega)$, and discretize the frequencies as follows:

$$\int_0^{\omega_j} d\omega\rho(\omega)=j,\quad j=1,\cdots,N. \tag{2.14}$$

We choose the density of frequencies as $\rho(\omega)=0.5N/\sqrt{\omega\omega_{\max}}$. The functional form of density does not affect the final result if enough bath modes are included. The discrete frequencies are $\omega_j=j^2\omega_{\max}/N^2$, $j=1,\cdots,N$. The maximum frequency $\omega_{\max}$ is set to be $20-200\omega_c$ depending on the specific parameters in the calculation. N is the degree of freedom of the bath. It is particularly useful to use the Debye spectral density ($J_D(\omega)=$

$\eta\omega\omega_c/(\omega^2+\omega_c^2)$), because it covers a broad frequency range. The coupling constant c_j for each frequency ω_j is given

$$c_j^2=\omega_j\frac{2}{\pi}\frac{J_D(\omega_j)}{\rho(\omega_j)}.$$

3 Numerical tests: The spin-boson model

In this case, a nonstationary quantum mechanical system is described by a two level system. Considering linear coupling of the two level system to a bath of harmonic oscillators. We take

$$h_S=\hbar\omega_0\sigma_x+\hbar\varepsilon\sigma_z, h_I=\sigma_z\otimes B, \tag{3.1}$$

where $\{\sigma_i\}_{i=x,y,z}$ are the standard Pauli matrices. In the spin-boson model, the numerical solution for the system density is equivalent to solving three non-linear coupled equations for the $\langle\sigma_i\rangle_S$.

The property of interest is the time evolution of the reduced density matrix in the two-state sub-system

$$\begin{aligned} &P_{i,j}(t)=\frac{1}{Q_B}tr[e^{-\beta\hat{H}_B}|1\rangle\langle 1|e^{i\hat{H}_t}|i\rangle\langle j|e^{-i\hat{H}_t}],\\ &Q_B=tr[e^{-\beta\hat{H}_B}], \end{aligned} \tag{3.2}$$

where $|i\rangle$ and $|j\rangle$ are the spin-state ($|1\rangle$ or $|2\rangle$), and the initial density matrix is set to spin-state $|1\rangle$ with a thermal distribution for the phonon bath. Expanding the Boltzmann operator in the bath eigenstates $|n\rangle$

$$e^{-\beta\widehat{H}_B}=\sum_n e^{-\beta E_n}|n\rangle\langle n|. \tag{3.3}$$

So $P_{i,j}(t)$ is rewritten as

$$\begin{aligned} P_{i,j}(t)&=\frac{1}{Q_B}\sum_n e^{-\beta E_n}\langle\Psi_n(0)|e^{i\hat{H}t}|i\rangle\langle j|e^{-i\hat{H}t}|\Psi_n(0)\rangle\\ &=\frac{1}{Q_B}\sum_n e^{-\beta E_n}\langle\Psi_n(t)|\,i\rangle\langle j\,|\Psi_n(t)\rangle, \end{aligned} \tag{3.4}$$

where we denote

$$|\Psi_n(0)\rangle=|1\rangle|n\rangle. \tag{3.5}$$

Following [29], we carry out the calculations for the time-dependent electronic population

$$P(t)\equiv\langle\sigma_z\rangle=\int dx_0\int dp_0 w(x_0,p_0)\left(\left|x^{(1)}_{x0,p0}\right|^2-\left|x^{(2)}_{x0,p0}\right|^2\right), \tag{3.6}$$

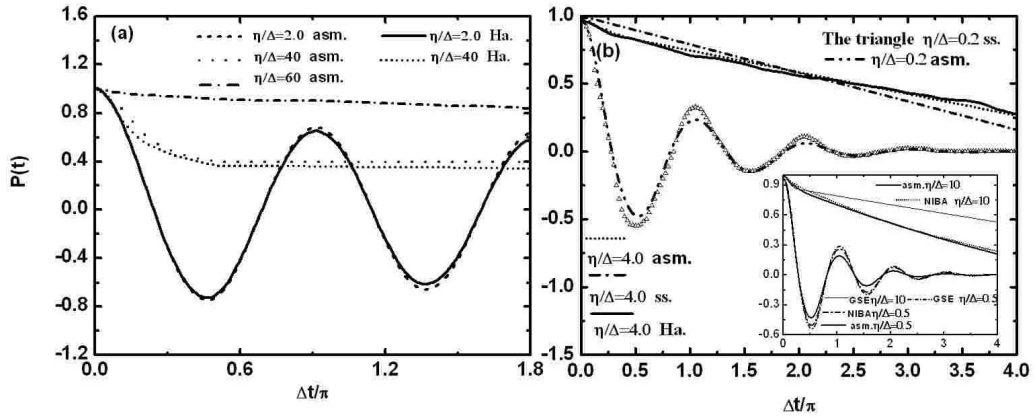

Figure 1: The population difference of the symmetric two-level system in (a) the adiabatic regime (Δ/ω_c=4) at $\beta\Delta$=2.0 (assuming $\langle\sigma_z(0)\rangle_s$=1). (b) the nonadiabatic regime (Δ/ω_c=0.2) at $\beta\Delta$=0.5 (assuming $\langle\sigma_z(0)\rangle_s$=1). Inset of fig(b) the nonadiabatic regime η/Δ=0.5 ,10.

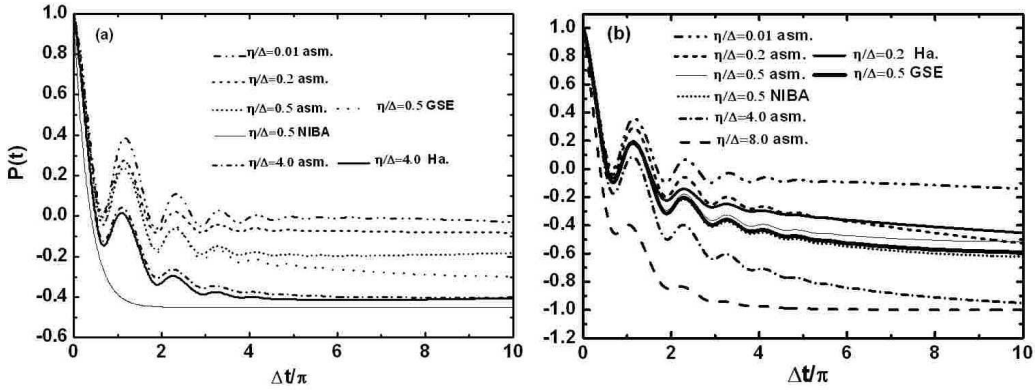

Figure 2: The population difference of the asymmetric two-level system at $\varepsilon/\Delta = 1$ and $\beta\Delta = 0.5$ for (a) η/Δ=0.01, 0.2, 0.5 and 4.0 in the adiabatic regime. (b) η/Δ=0.01, 0.2, 0.5, 4.0 and 8.0 in the nonadiabatic regime.

which is evaluated by solving numerically the electronic equations of motion, chosen according to the electronic initial conditions as $x^{(1)}_{x0,p0} = 1$ and $x^{(2)}_{x0,p0} = 0$. $w(x_0,p_0)$ refers to the classical trajectory with initial conditions x_0 and p_0. The function $w(x_0,p_0)$ thus represents the initial distribution of the environment. The averaged semiquantum method provides an alternative way to study the open quantum systems dynamics. Much less trajectories seem to be needed to accurately describe the dynamical evolution. Only 20000 trajectories have been used to obtained Figs. 2 and 3. The computer time for the two figures was less than an hour in the weak coupling and low temperature case up to several hours in the strong coupling and high temperature case. This was caused by the time step Δt. In order to obtain accurate results, $\Delta t\omega_0 = 1.0\times10^{-3}$ and $\Delta t\omega_0 = 1.5\times10^{-4}$ have been used for weak coupling and low temperature case and strong coupling and high temperature case respectively.

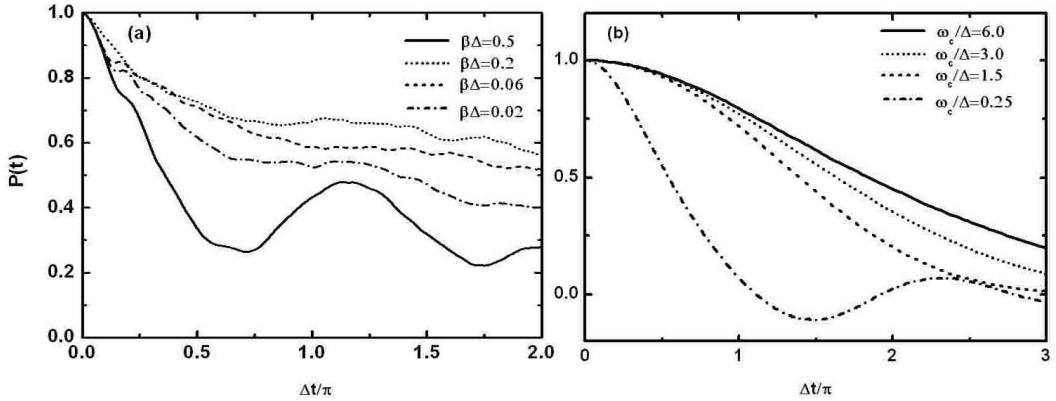

Figure 3: The population difference at (a) η/Δ=0.1 and Δ/ω_c=4 with different temperature, (b) η/Δ=10and $\beta\Delta$=0.2 with different ω_c.

Fig. 1 shows the population difference of the symmetric two-level system for different parameters in both the adiabatic and nonadiabatic regimes at relatively low and high temperatures respectively. Results can be compared with those from the Hierarchical approach (Ha.) proposed in [30] (see Figs. 2 and 3) or stochastic simulation (ss) in [16] (see Fig. 1). We also compare our results with NIBA results and GSE results. In general, NIBA is a rather good approximation for nonadiabatic electron transfer, in particular for systems without electronic bias. These figures display the tendency for transitions from coherent to incoherent motion as the coupling strength increases. Fig. 1(a) shows the averaged semiquantum results (asm) for three different couplings. The parameters used in the calculation are $\beta\Delta = 2.0$ and $\Delta/\omega_c = 4.0$. For the smallest coupling in the figure, $\eta/\Delta = 2$, the averaged semiquantum method predicts coherent dynamics, and agrees well with the Hierarchical approach. When $\eta/\Delta = 40$, our method predicts incoherent relaxation, after a short transient time. For the largest coupling in Fig. 1(a), η/Δ=60, the result also agrees well with the Hierarchical approach's prediction. Similarly, Fig. 1(b) displays the population difference of the symmetric two-level system in the nonadiabatic regime. We set the parameters $\beta\Delta = 0.5$ and $\Delta/\omega_c = 0.2$. Inset of Fig. 1(b) shows that NIBA agrees with the results of asm over the whole range of coupling strengths. The GSE can also reproduce the weak-coupling result very well for small coupling strength. If the coupling strength η/Δ is increased, the results of GSE break down. It is because that the temperature is high compared to the characteristic frequency of the bath ω_c is not fulfilled here ($\beta\omega_c$=2.5) [43].

Results of numerical simulations of an asymmetric $\varepsilon \neq 0$ two level system at a finite temperature are shown in Fig. 2. The results are found to be in a qualitative agreement with the Hierarchical approach [30] (see Fig. 4), which show a transition from coherent oscillatory dynamics to relaxation with increasing system-bath coupling. From Fig. 2, we have found that $P(t)$ decrease to different saturated values with different η/Δ. The larger η/Δ, the more rapid $P(t)$ decreases. For the small coupling, η/Δ=0.01, $P(t)$ decreases to

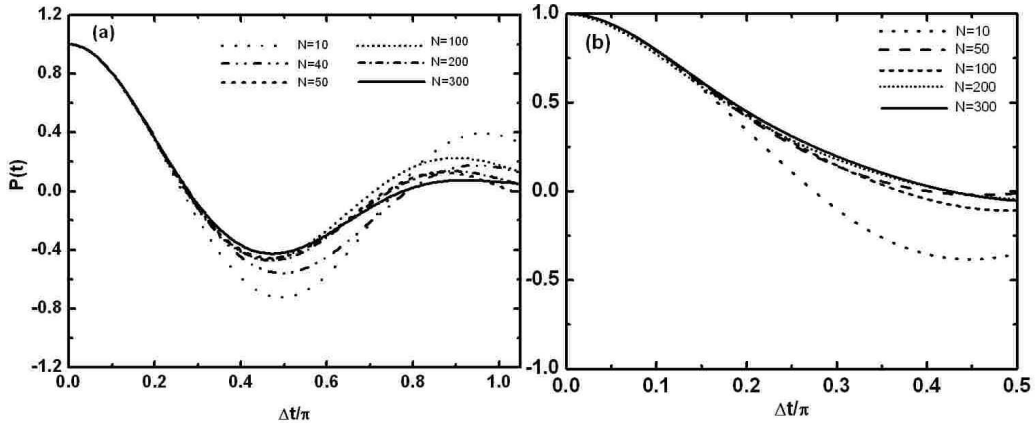

Figure 4: The population difference of the symmetric two-level system in the nonadiabatic and the adiabatic regime with different bath-dimensionality.

-0.13 slowly. For the larger couplings, $\eta/\Delta=0.2$,0.5, and 4.0, the saturated value is about $-0.09,-0.18$, and -0.4 respectively. For a moderate coupling strength $\eta/\Delta=0.5$, NIBA gives qualitatively incorrect results in this parameter regime. It is also known that NIBA breaks down in biased systems for an Ohmic spectral density. However, the GSE is in good agreement with the simulation. We next turn to the nonadiabatic regime. Fig. 2(b) shows the result for high temperature. For the largest coupling, $\eta/\Delta=8.0$, $P(t)$ decreases to -1 quickly. All approximate methods we have tested reproduce the dynamics qualitatively correctly.

At low temperature, the total number of states accessible for the bath is limited and so is energy exchange between the system and the bath. As the temperature increases, more bath states participate in the energy transfer process, which tends to destroy the coherent motion of the two level system. Fig. 3(a) shows $P(t)$ for different temperatures (here we use $\beta\Delta$ as a measure of temperature). The other parameters are $\eta/\Delta=5$ and $\Delta/\omega_c=4$. At low temperature, $\beta\Delta=0.5$, there is a strong coherent character in $P(t)$. The coherent component becomes less for a higher temperature of $\beta\Delta=0.2$, and there is barely any coherence left for the still higher temperature of $\beta\Delta=0.06$. At the highest temperature, $\beta\Delta=0.02$, $P(t)$ displays totally incoherent dynamics. Fig. 3(b) shows$P(t)$ at $\eta/\Delta=10$ and $\beta\Delta=0.2$, for several ω_c's. The trend is clear: $P(t)$ shows strongly coherent character for the small ω_c. The coherence becomes less prominent as ω_c/Δ increases to 1.5, and almost disappears for $\omega_c/\Delta=3$. For $\omega_c/\Delta=6$, $P(t)$exhibits complete incoherent dynamics. This transition is also caused by the bath. When ω_c starts from a small value, the frequencies of bath are also restricted to small values. The relaxation of bath is very slow, and unable to destroy the coherent motion of the two-level system. As ω_c increases larger, the response of bath becomes faster so that the bath can participate in the decoherence. When ω_c is large enough, $P(t)$ decreases all the time, also caused by the interaction between the bath and the two level system.

From Eq. (2.7), we can find that the value of Δq decreases with the increase of the tem-

perature. The value of $N_k$was less than 50 in the high temperature case up to more than 100 for the low temperature case. In order to obtain accurate results, we choose suitable values of Δq to reduce statistical error for different initial conditions. In the low temperature regime, we choose $\Delta q = \frac{0.02*\hbar}{m_k\omega_k}$, while $\Delta q = \frac{0.1*\hbar}{m_k\omega_k}$ for higher temperature. For low temperatures and small cutoff frequency, the value of $\langle B\rangle$remains close to zero during the whole evolution. The situation changes for large cutoff frequency, in which $\langle B\rangle$ reaches greater amplitude of fluctuations, producing a noise distant from zero. Furthermore, the behavior of $\langle B\rangle$ is like the real noise. For high temperatures, the amplitude of fluctuations comes to a larger value. Under low temperature and small cutoff frequency condition, the trajectory of bath is almost regular. The situation at large cutoff frequency is different. The trajectory is completely chaotic. When the values of ω_c and temperature are large, the dynamic of bath is not only chaotic, but also spreads to a much bigger region.

From the above discussion, we have found that the bath at large ω_c and high temperature is chaotic and can produce enough noise, taking part in the decoherence. The system is insensitive to the details of the heat bath. In other words, the statistical properties of system depend on the temperature, cutoff frequency and degree of freedom of the bath. When most initial states of bath are located in the regular islands, the manner of decoherence shows an oscillatory behavior. When the bath is completely chaotic, it can produce enough noise to eliminate the quantum interference, and turns the manner of decoherence from oscillatory to always decrease.

Furthermore, we want to study the effects of the bath-dimensionality on the population difference. In Fig. 4 results are plotted for a symmetric bath with different dimensionality. Panel (a) shows the case of medium electronic coupling in the nonadiabatic regime ($\Delta/\omega_c = 0.2$) at $\beta\Delta = 0.5$, $\eta/\Delta = 1$ (assuming $\langle\sigma_z(0)\rangle_s = 1$). Panel (b) shows the case of strong electronic coupling in the adiabatic regime ($\Delta/\omega_c = 4$) at $\beta\Delta = 2.0$, $\eta/\Delta = 20$ (also assuming $\langle\sigma_z(0)\rangle_s = 1$). Note that the agreement between the results and the exact one (solid line) seems to improve with increasing dimensionality. For the small bath-dimensionality, there are obvious differences compared with the accurate results. When $N = 100$, there is almost no difference between the result and the real case (solid line). So it is sufficient for choosing $N = 300$ to perform the calculations above.

In Fig. 5, $P(t)$ are depicted by varying δ (nonequilibrium parameter). As expected, the decoherence occurs immediately, in sharp contrast to equilibrium case. $P(t)$ shows strongly coherent character at first for $\delta = 0$, as shown in Fig. 5(a). The coherence becomes less prominent as $\delta = 0$ is increased to $\delta = 1$ and 4 and has almost disappeared for $\delta = 8$. For $\delta = 15$,30,80, $P(t)$ exhibits complete incoherent dynamics, where the system is in a nonequilibrium environment (Fig. 5(a)). Not only in symmetric two-level system but also asymmetric two-level system, a notable difference between equilibrium environment and the case of $\delta \neq 0$ can be observed, as shown in Fig. 5(b). The saturated value of $P(t)$ is also decreasing with the increase of δ, while it is almost unchanged at a somewhat larger δ, shown in Fig. 5(b). The increase of nonequilibrium parameter can not only provides a large noise, but also produces great amplitude of fluctuations. The noise destroys the quantum interference and lets nondiagonal matrix element decrease.

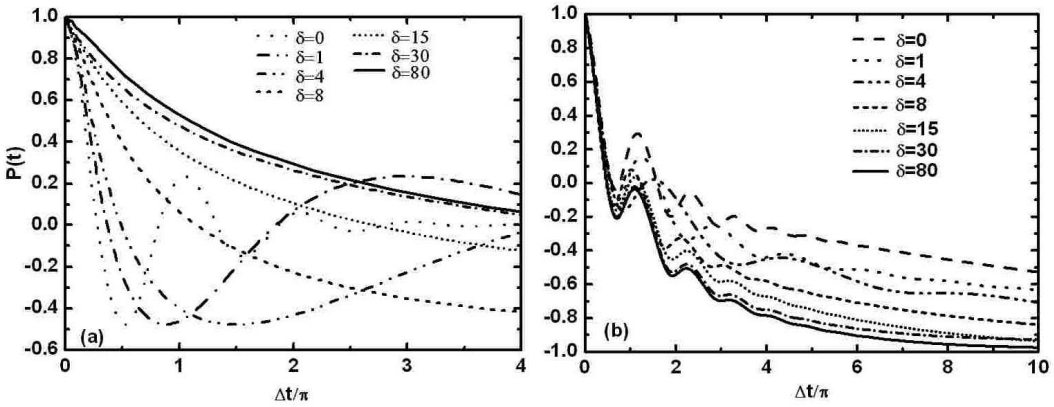

Figure 5: Panel (a) shows the population difference of the symmetric two-level system in the adiabatic regime ($\Delta/\omega_c=4$) at $\beta\Delta=2.0$ (assuming $\langle\sigma_z(0)\rangle_s=1$), with different δ. Panel (b) shows the population difference of the asymmetric two-level system at $\varepsilon/\Delta=1$and $\beta\Delta=0.5$, with different nonequilibrium parameters.

4 Numerical tests: A harmonic oscillator coupled to bath

Following [31], the area covered by the wave packet is related to the linear entropy through

$$s(\rho)=1-\frac{1}{A}. \tag{4.1}$$

The "area" A in the two-dimensional phase space is given in units of Planck's constant. The linear entropy is increasing functions of A, which can be computed as a function of time and has the following simple overall form (see Ref. [32] for technical details):

$$A=\{A_0^2+A_0[sf_+(t)+s^{-1}f_-(t)]+h(t)\}^{1/2}, \tag{4.2}$$

where the initial area $A_0=2\Delta x\Delta p/\hbar$ and the squeezed parameter $s=m\omega\Delta x\Delta p$ parameterize the initial state, while $f_\pm$ and h are complicated functions of time and temperature. To verify the key result, we compute for an initially pure state (Gaussian wave packet).

Let us first look at decoherence for different coupling strengths and temperatures with various N, displayed in Figs. 6 and 7 respectively. As expected, the decoherence occur for various conditions. In contrast to the master equations case, the entropy increase can reproduce the similar results for large N. When N is small, there are few initial bath states take part in the decoherence. With N increasing, more bath states are considered. So it is close to the real case. At low temperature and small coupling strength, D saturates at a value considerably away from one. In Fig. 6, the saturated value gradually increases with the increase of the coupling strength. Only at the largest coupling strength, in Fig. 6(d), the saturated value is close to one. The average nondiagonal matrix element is almost equal to zero. Similar effects are seen in Fig. 7 with the different temperature. The saturation values are obviously growing with the increase of N, until up to 70. So $N=80$ is sufficient to describe the bath. The curve of decoherence function is almost unchangeable for further increase N.

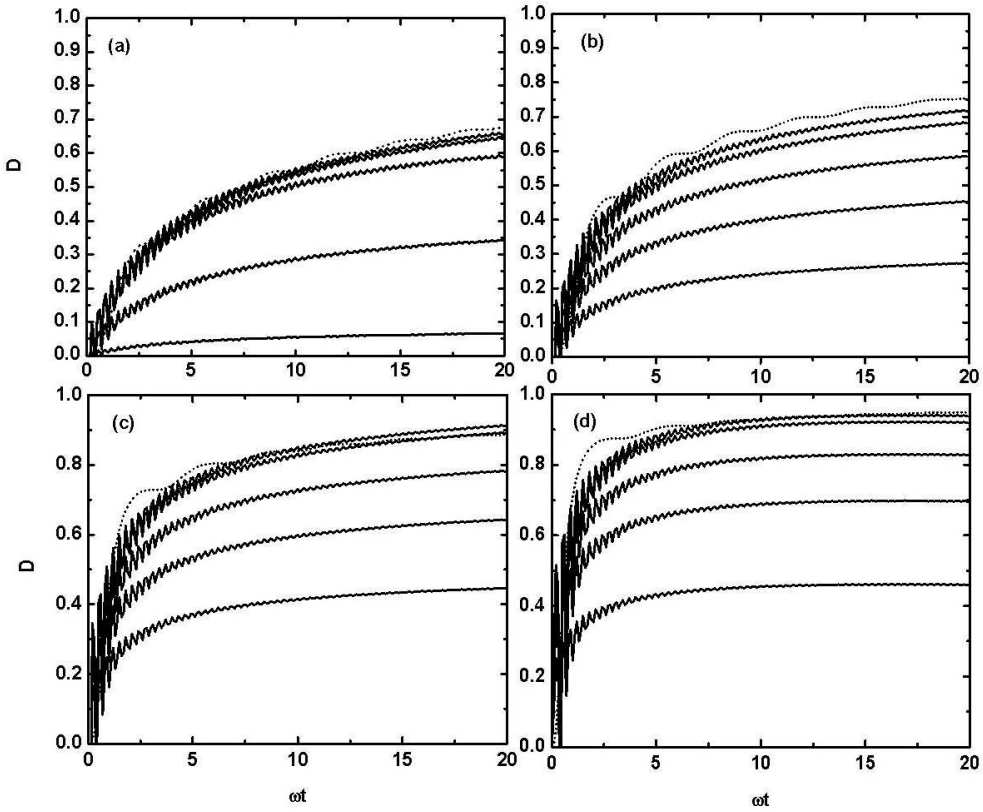

Figure 6: D vs time. Results compared with the master equations' results (dot line) with different coupling strength, from bottom to top,N=20, 36, 50, 70, 80. T=20. (a) η=0.01. (b) η=0.05. (c) η=0.08. (d) η=0.1.

In Fig. 8, the same quantity D is depicted at a fixed coupling strength, but varied temperatures. Of course, pronounced decoherence is seen for fixed N=80, where the system is in a nonequilibrium environment. Now an obvious difference between equilibrium environment and the case of $\delta \neq 0$ can be observed. Even for weak coupling and low temperature, the decoherence function is increasing, with increasing centers shifted towards the equilibrium point of the bath. The saturated value of D is also increasing with the increase of δ, while it is almost changeless at a somewhat larger δ. Let us first look at decoherence for small coupling strength and low temperature with different δ, displayed in Fig. 8(a). As expected, the decoherence occurs immediately, in sharp contrast to equilibrium case. At higher temperature, the saturated value is in different extent of closing to one, shown in Fig. 8(b). Thus revealing the substantial influence of δ. This influence gradually decreases when the nonequilibrium parameter is larger. The result, at the δ=30, is almost consistent with the case at the largest δ=40. Further, we consider why the nonequilibrium parameter has effects on the decoherence. When $\delta \neq 0$, the bath gives a larger $\langle B \rangle$. The value remains close to δ during the whole evolution. The situation changes for large δ, in which $\langle B \rangle$ reaches greater equilibrium of fluctuations, producing

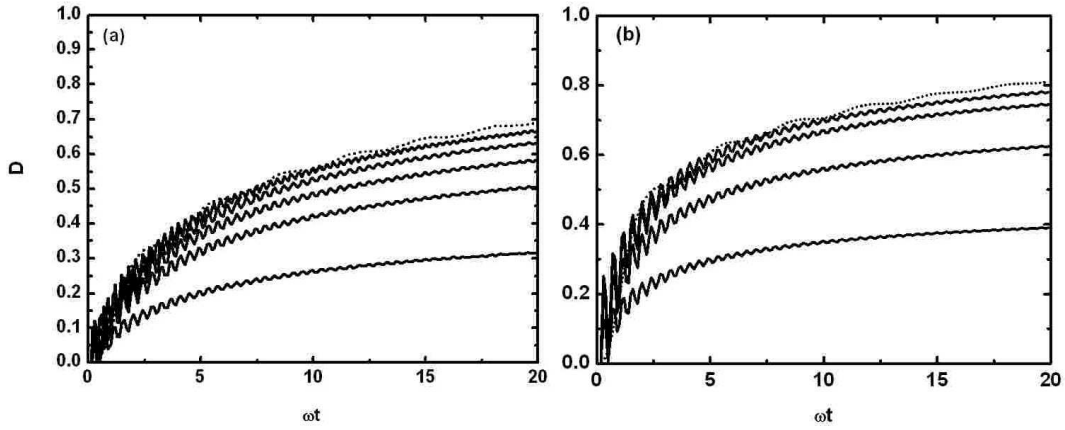

Figure 7: D vs time. Results compared with the master equations' results (dot line) with different temperature, $\eta=0.1$, from bottom to top, N=20, 36, 50, 70, 80. (a) $T=5$. (b) $T=10$.

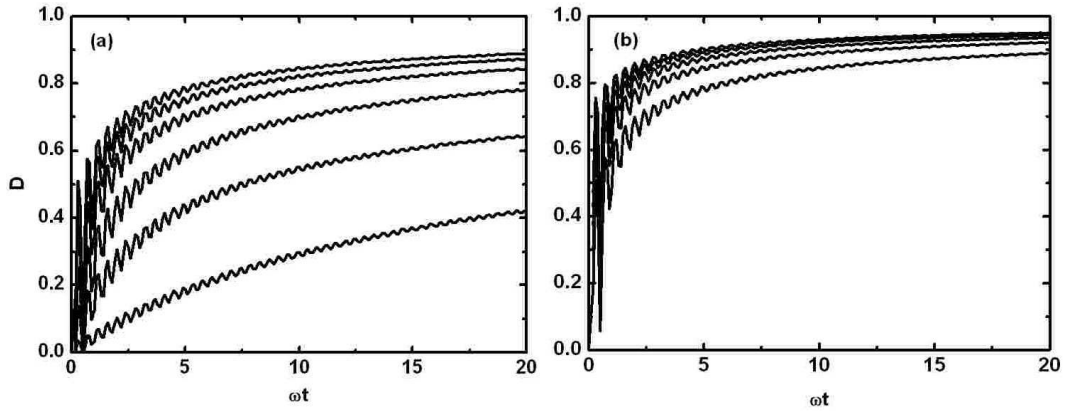

Figure 8: D vs time. Results in nonequilibrium environment with different δ, from bottom to top, δ=5, 10, 20, 30, 40. $\eta=0.08$. (a) $T=5$. (b)$T=20$.

a noise distant from δ. The increase of nonequilibrium parameter can provide a large noise. The noise destroys the quantum interference and let nondiagonal matrix element decrease. We are inside the weak coupling regime in the sense of master equations. To check the thermal nature of the final values, we used initial condition sampling. The total number of sampling points needed to generate all presented results is 12000; the calculations take a few hours on a desktop PC.

In general case, the time evolution of quantum state $\rho(t)$ is described by Liouville-von Neumann equation

$$\frac{d}{dt}\rho_t=\widehat{\Lambda}\rho_t,$$

where $\widehat{\Lambda}$ is a quantum Liouville operator. Stationary state is defined by the condition $\widehat{\Lambda}\rho_t=0$. The system interacts with bath only through the mean field $\langle B(t)\rangle_E$. The dissipa-

tion drives the model system to a stationary state. In the case of a thermal reservoir, this final state should be a thermal equilibrium state. In most applications,

$$\rho_B = Z_\beta^{-1} e^{-\beta H_B}$$

is a thermal state at the inverse temperature $\beta=(k_B T)^{-1}$ with the normalization constant Z_β. In the presentations of Figs. 5 and 8, it indicates that a stationary state has been reached as $t\to\infty$. The averaged Gaussian wave function (2.4), (2.5) is easily verified by checking that $\rho(t)$ also satisfies the expectation value of the quantum Liouville equation. As $t\to\infty$, the final evolution has no relation to the coupling potential. A true stationary state does exist, when $<B>=0$. In both the spin-boson and harmonic oscillators model, the numerical evolution of $<B>$, beginning from an unstable initial state, does go to zero at late times.

To confirm that the semiquantum method can predict decoherence, following [33–34], we illustrate numerically the decoherence of a superposition of two symmetrically located coherent states, which have been intensively investigated by master equation. The Hamiltonian of this system is

$$h_S = \frac{p_s^2}{2m_s} + \frac{1}{2} m_s \omega_0^2 q_s^2, \quad h_I = q_s \sum_{i=1}^{N} \lambda_i q_s. \tag{4.3}$$

And the environment is a heat bath of oscillators. Our aim is to illustrate various decoherence scenarios for quantum superposition $|\varphi\rangle = c_1|\varphi_1\rangle + c_2|\varphi_2\rangle$ by using semiquantum method. We choose coherent states with uncertainty $\Delta q \Delta p = \hbar/2$. To ensure good separation, we stipulate that either $\Delta q \ll |q_1 - q_2|$ or $\Delta p \gg |p_1 - p_2|$, which assumes $\langle \varphi_1 | \varphi_2 \rangle \approx 0$. $d_Q = |q_1 - q_2|$ denotes the separations in position of the two wave packets. The initial density operator is a sum of four terms,

$$\rho_{sys}(0) = \sum_{i,j=1}^{2} c_i c_j^* |\varphi_i\rangle \langle \varphi_j| = \sum_{i,j} c_i c_j^* \rho_{sys}^{ij}(0),$$

and two off-diagonal interference terms are

$$\rho_{sys}^{12}(0) = |\varphi_1\rangle \langle \varphi_2| = \rho_{sys}^{21}(0)^+.$$

In [33–34], the authors employ the norm

$$N_{12}(t) = Tr_{sys} \rho_{sys}^{12}(t) \rho_{sys}^{21}(t)^+$$

as an indictor of the temporal fate of the relative coherence between the two superposed wave packets. Clearly, if the system were closed, its unitary time evolution would leave that norm constant in time ($N_{12}(t)=1$); interaction with a many-freedom environment will cause decay.

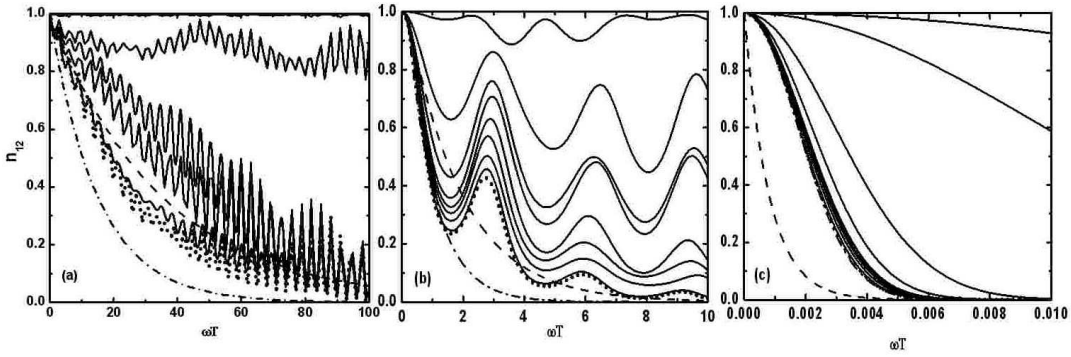

Figure 9: n_{12} vs time. Dash line: golden-rule result. Dash dot line: interaction-dominance results. Solid lines: averaged semiquantum results. From top to bottom, (a) N=20, 36, 50, 70, 80(dot). $d_Q=16$. (b) N=5, 10, 20, 30, 40, 50, 60, 70, 80 (dot). $d_Q=80$. (c) N=2, 5, 10, 20, 30, 50, 60, 70, 80 (dot). $d_Q=4000$.

Similarly to the $N_{12}(t)$, we employ the norm $n_{12}(t)=Tr_{sys}\rho^{12}_{sys}(t)\rho^{21}_{sys}(t)^{+}$ to measure the relative coherence between the two superposed wave packets. If the system interact with a many-freedom environment,

$$\begin{aligned} n_{12}(t) &= \left\langle \bar{\phi}^B_2(t) \middle| \bar{\phi}^B_1(t) \right\rangle \left\langle \bar{\phi}^B_1(t) \middle| \bar{\phi}^B_2(t) \right\rangle \\ &= \prod_n \exp\left(-0.5(\bar{q}_{1n}(t)-\bar{q}_{2n}(t))^2/\bar{G}_n - 0.5\bar{G}_n(\bar{p}_{1n}(t)-\bar{p}_{2n}(t))^2/\hbar^2\right). \end{aligned} \tag{4.4}$$

We choose that cutoff frequency equals to 100Ω and $\omega_i \in [1,100]$ obtained from uniform random number, and approximate the thermal energy by sampling from a classical canonical distribution and let the thermal energy equals to $20\hbar\Omega$. Furthermore, we compare our results obtained by semiquantum method with the results from master equation.

In Fig. 9, we show the decay of n_{12} of initial superposition with different separation (d_Q). The dash and dash dot lines show the golden-rule result and interaction-dominance result. The solid lines show the semiquantum numerical results with different dimensionality. When $d_Q=16$, the saturated value of n_{12} is about 0.88 at N=20. The decay of n_{12} changes from saturated to linear at N=36, and from linear to exponential with the increase of the dimensionality N=70, which is close to the golden-rule results. When $N\geq 80$, the trend of the decay is almost changeless. In Figs. 9(b) and 9(c), we also show the decay of n_{12} with separation $d_Q=80$ and $d_Q=4000$ with different dimensionality, and find that the n_{12} decreases more quickly with the increase of N. The decay of n_{12} is almost unchanged, when $N\geq 70$ in Fig. 9(b) and when $N\geq 30$ in Fig. 9(c). The critical value of N decreases with the increase of the d_Q, when the decay is stable. Furthermore, we also find the various decoherence scenarios: golden-rule, crossover, and interaction-dominated regime. At $d_Q=16$ and $N=80$, the semiquantum result is close to the golden-rule. When $d_Q=80$ and $N\geq 70$, the results are between the golden-rule line and interaction-dominance line. For $d_Q=4000$ and $N\geq 30$, the full line fits the interaction-dominance line well. These results not only agree with those obtained by master equation method, but also show how

the dimensionality of the external system affects on the relative coherence between the two superposed wave packets.

5 Conclusion

The results obtained from the averaged semiquantum method for the harmonic oscillators and the spin-boson model are very encouraging. This method turns out to be useful not only to simulate short-time but also long-time dynamics. Furthermore, it can be used to solve the problem, nonequilibrium environment. Choosing suitable initial values can reduce the number of paths and the freedom of the bath. We presented specific applications on systems coupled to a heat bath with different coupling strengths and temperatures. The semiquantum method agrees with not only the prediction of master equation but also many other quantum methods (stochastic equation, Hierarchical approach and so on).

It is worth mentioning that the evolvement of the bath is governed by the dynamic equation with no approximation, which is very close to the real case. So this approach can be applied to various types of model ($H=h_S+h_E+h_I$), which is a useful tool to study dissipation, measurement and decoherence problems in quantum systems and to study the quantum-classical transition in the high-dimensional model.

Acknowledgments

This work is supported by the National Science Foundation (Grant Nos. 1037504 and 10875087).

Appendix: Generalization to the averaged semiquantum method

In this appendix, we discuss the generalization of the averaged semiquantal dynamics to N dimensional model. For the general case, we consider all the correlations between the various degrees of freedom. The best way to derive the equations of motion in this case is to use the a wave packet of the form

$$\psi(x,t)=\exp\left[\frac{i}{\hbar}[(x-q)\cdot A\cdot(x-q)+p\cdot(x-q)]\right], \tag{A.1}$$

where x,p,q are vectors and A is a symmetric $N\times N$ matrix. We rewrite A as $A=i\frac{1}{4}G^{-1}+\Pi$ with G,Π real symmetric matrices. The initializations of the vectors p,q and the real symmetric matrices G,Π are according to the equation (2.6). We can obtain the extended Hamiltonian

$$H_{ext}=\frac{1}{2}p^2+V(x)+Tr\left(\frac{1}{8}G^{-1}+\Pi^2G+G\Pi^2\right)+\langle V(x)\rangle, \tag{A.2}$$

where *Tr* indicates the trace operation on the matrices. The only calculation of any subtlety is the evaluation of $\langle V(x)\rangle$, since $\psi(x)$is a multivariate Gaussian distribution. We consider a system (S)-environment (E) described by a Hamiltonian

$$H=h_S+h_E+h_I, \tag{A.3}$$

The interactions between the various degrees of freedom of bath are ignored. So we can simple wave packet (Eq. (A1)) into the form $|\psi\rangle=|\psi_0\rangle\prod_{k=1}^{N}|\psi_k\rangle$. We can obtain the equations of motion directly by time-dependent variational principle (TDVP) formulation, $\Gamma=\int dt\langle\Psi(t)|i\hbar\frac{\partial}{\partial t}-\hat{H}|\Psi(t)\rangle$ with $\delta\Gamma=0$. We solve the integrable multidimensional function $\langle\Psi(t)|i\hbar\frac{\partial}{\partial t}-\hat{H}|\Psi(t)\rangle$ and obtain the analytic results, since $\psi(x)$ is a multivariate Gaussian distribution. Then using $\delta\Gamma=0$, we can get the equations of motion for each trajectories. For spin-boson model, $|\psi_0\rangle$ is written as

$$|\psi_0\rangle=(A+iB)|0\rangle+(C+iD)|1\rangle, \tag{A.4}$$

Moreover, as the influence of the environment on the system only enters through

$$\langle B(t)\rangle_E=-\sum k_n\left\langle q_{(}t)\right\rangle,$$

the introduction of the mean field to the interaction simplifies the version of the coupled model. Then, we can obtain the averaged semiquantum method working equations:

$$\begin{aligned}
&\dot{A}=2.0*\omega_0*D+2.0*\varepsilon*B+2.0*\langle B(t)\rangle_E*D,\\
&\dot{B}=-2.0*\omega_0*C-2.0*\varepsilon*A-2.0*\langle B(t)\rangle_E*C,\\
&\dot{C}=2.0*\omega_0*B-2.0*\varepsilon*D+2.0*\langle B(t)\rangle_E*B,\\
&\dot{D}=-2.0*\omega_0*A+2.0*\varepsilon*C-2.0*\langle B(t)\rangle_E*A.
\end{aligned} \tag{A.5}$$

For harmonic oscillators model, we represent $|\psi_0\rangle$ as the Gaussian wave packet and we can get the equations of motion for each trajectories, ignoring the interactions between the various degrees of freedom of bath:

$$\begin{aligned}
&\frac{dq_k}{dt}=\frac{\partial H_{ext}}{\partial p_k},\quad \frac{dp_k}{dt}=-\frac{\partial H_{ext}}{\partial q_k},\\
&\frac{dG_k}{dt}=\frac{\partial H_{ext}}{\partial \Pi_k},\quad \frac{d\Pi_k}{dt}=\frac{\partial H_{ext}}{\partial G_k}.
\end{aligned} \tag{A.6}$$

We average the physical parameter $(q_k,p_k,G_k,\Pi_k,\cdots)$ to calculate our interested quantities to measure decoherence.

References

[1] U. Weiss, Quantum Dissipative System, World Scientific Singapore, 1993.

[2] M. Grifoni and P. Hanggi, Driven quantum tunneling, Phys. Rep., 304 (1998), 229-354.
[3] H. P. Breuer and F. Petruccione, The Theory of Open Quantum Systems, Oxford University Press, 2002.
[4] G. Wendin and V. S. Shumeiko, Quantum bits with Josephson junctions, Low Temp. Phys., 33 (2007), 724.
[5] C. M. Tesch and R. de. Vivie-Riedle, Quantum Computation with Vibrationally Excited Molecules, Phys. Rev. Lett., 89 (2002), 157901.
[6] W. H. Zurek, Decoherence and the transition from quantum to classical, Phys. Today, 44 (1991), 36-44.
[7] S. Krempl, M. Winterstetter, H. Plohn and W. Domcke, Path-integral treatment of multi-mode vibronic coupling, J. Chem. Phys., 100 (1994), 926.
[8] J. Dalibard, Y. Castin and K. Mølmer, Wave-function approach to dissipative processes in quantum optics, Phys. Rev. Lett., 68 (1992), 580-583.
[9] R. Dum, P. Zoller and H. Ritsch, Monte Carlo simulation of the atomic master equation for spontaneous emission, Phys. Rev. A, 45 (1992), 4879.
[10] N. Gisin and I. Percival,The quantum-state diffusion model applied to open systems, J. Math. Phys. A, 25 (1992), 5677-5691.
[11] H. Carmichael, An Open Systems Approach to Quantum Optics, Lecture Notes in Physics, Springer-Verlag, Berlin, 1993.
[12] Y. Castin and K. Mølmer, Monte Carlo wave functions and nonlinear master equations, Phys. Rev. A, 54 (1996), 5275.
[13] M. Rigo and N. Gisin, Unravellings of the master equation and the emergence of a classical world, Quantum Semiclass. Opt., 8 (1996), 255-68.
[14] W. Gardiner and P. Zoller, Quantum Noise, Springer-Verlag, Berlin-Heidelberg, 2000.
[15] H. P. Breuer and F. Petruccione, Numerical integration methods for stochastic wave function equations, Comput. Phys. Commun., 132 (2000), 30-43.
[16] D. Lacroix, Stochastic simulation of dissipation and non-Markovian effects in open quantum systems, Phys. Rev. E, 77 (2008), 041126.
[17] D. Lacroix, Optimizing stochastic trajectories in exact quantum-jump approaches of interacting systems, Phys. Rev. A, 72 (2005), 013805.
[18] C. W. Gardiner, Handbook Of Stochastic Methods Second Edition,Springer, 1992;W. T. Strunz, L. Diósi, N. Gisin and T. Yu, Quantum Trajectories for Brownian Motion, Phys. Rev. Lett., 83 (1999), 4909-4913; J. T. Stockburger and H. Grabert, Exact c-Number Representation of Non-Markovian Quantum Dissipation, Phys. Rev. Lett., 88 (2002), 170407.
[19] W. V. Liu and W. C. Schieve, Quantum Chaotic Attractor in a Dissipative System, Phys. Rev. Lett., 78 (1997), 3278-81;A. K. Pattanayak and W. C. Schieve, Calculation of eigenvalues of a strongly chaotic system using Gaussian wave-packet dynamics,Phys. Rev. E, 56 (1997), 278-284.
[20] B. Hu, B. Li and J. L. Zhou, Squeezed state dynamics of kicked quantum systems, Phys. Rev. E, 58 (1998), 1743-56.
[21] A. K. Pattanayak and W. C. Schieve, Gaussian wave-packet dynamics: Semiquantal and semiclassical phase-space formalism, Phys. Rev. E, 50 (1994), 3601-3615.
[22] R. Jackiw and A. Kerman, Time-dependent Variational Principle and the Effective Action, Phys. Lett., 71A (1979), 158.
[23] Y. Tsue and Y. Fujiwara, Time-Dependent Variational Approach in Terms of Squeezed Coherent States, Pro. Theor. Phys., 86 (1991), 443-467.
[24] B. Hu and B. Li, Quantum Frenkel-Kontorova Model, Phys. A., 288 (2000), 81-97.

[25] W. H. Zurek, Decoherence, einselection, and the quantum origins of the classical, Rev. Mod. Phys., 75 (2003), 715-75.
[26] O. V. Prezhdo and P. J. Rossky, Relationship between Quantum Decoherence Times and Solvation Dynamics in Condensed Phase Chemical Systems, Phys. Rev. Lett., 81 (1998), 5294.
[27] E. J. Heller, 1981 Frozen Gaussians: A very simple semiclassical approximation, J. Chem. Phys., 75 (1998), 2923.
[28] O. V. Prezhdo and P. J. Rossky, Evaluation of quantum transition rates from quantum-classical molecular dynamics simulations, J. Chem. Phys., 107 (1997), 5863.
[29] U. Peskin and M. Steinberg, A temperature-dependent Schrödinger equation based on a time-dependent self consistent field approximation, J. Chem. Phys., 109 (1998), 704; G. Stock, A semiclassical self-consistent-field approach to dissipative dynamics: The spin–boson problem, J. Chem. Phys., 103 (1995), 1561; A. A. Golosov, R. A. Friesner and P. Pechukas, Reduced dynamics in spin-boson models: A method for both slow and fast bath, J. Chem. Phys., 112 (2000), 2095; H. Wang, X. Song, D. Chandler and W. H. Miller, Semi-classical study of electronically nonadiabatic dynamics in the condensed-phase: Spin-boson problem with Debye spectral density, J. Chem. Phys., 110 (1998), 4828.
[30] Y. Yan, F. Yang, Y. Liu and J. Shao, Hierarchical approach based on stochastic decoupling to dissipative systems,Chem. Phys. Lett., 395 (2004), 216.
[31] W. H. Zurek, S. Habib and J. P. Paz, Coherent states via decoherence, Phys. Rev. Lett., 70 (1993), 1187-1190.
[32] J. P. Paz, S. Habib and W. H. Zurek, Reduction of the wave packet: Preferred observable and decoherence time scale, Phys. Rev. D, 47 (1993), 488-501.
[33] W. T. Strunz and F. Haake, Universality of decoherence for macroscopic quantum superpositions, Phys. Rev. A., 67 (2003), 022101.
[34] W. T. Strunz and F. Haake, Decoherence scenarios from microscopic to macroscopic superpositions, Phys. Rev. A., 67 (2003), 022102.
[35] A. J. Leggett, S. Chakravarty, A. T. Dorsey, M. P. A. Fisher, A. Garg and W. Zwerger, Rev. Mod. Phys., 59 (1987), 1.
[36] C. Aslangul, N. Pottier, and D. Saint-James, J. Phys.(Paris), 47 (1986), 1657.
[37] L. Zusman, Chem. Phys., 49 (1980), 295.
[38] A. Garg, J. Onuchic, and V. Ambegaokar, J. Chem. Phys., 83 (1985), 4491.
[39] L. Hartmann, I. Goychuk, and P. Hänggi, J. Chem. Phys., 113 (2000), 11159.
[40] A.J. Leggett, S. Chakravarty, A. T. Dorsey, M. P. A. Fisher, A. Garg and W. Zwerger, Dynamics of the dissipative two-state system, Rev. Mod. Phys., 59 (1987), 1-85; ibid. 67 (1995), 725.
[41] H. Grabert, P. Schramm and G.-L. Ingold, Quantum Brownian Motion: The Functional Integral Approach, Phys. Rep., 168 (1988), 115-207.
[42] E. Neria and A. Nitzan, Semiclassical evaluation of nonadiabatic rates in condensed phases, J. Chem. Phys., 99 (1993), 1109.
[43] M. Thoss, H. Wang and W. H. Miller, Self-consistent hybrid approach for complex systems: Application to the spin-boson model with Debye spectral density, J. Chem. Phys., 115 (2001), 2991.